Effect of Simulated Mission Loads on Orbiter Thermal Protection System Undensified Tiles

Paul A. Cooper,* Robert Miserentino,† James Wayne Sawyer,‡ and Jack D. Leatherwood§
NASA Langley Research Center, Hampton, Virginia

The Thermal Protection System (TPS) used on the undersurface of the Shuttle Orbiter consists of several thousand ceramic tiles bonded to sections of low modulus felt material, which are in turn individually bonded to the aluminum skin of the Orbiter. The TPS exhibited low strength at the interface between the tile and the strain isolation pad. Tiles failing a tensile proof test were removed and strengthened by applying a ceramic slurry which provided a densified region at the bonding surface. Because of cost and schedule considerations, many tiles which passed the proof test were not removed and densified before the first Shuttle flight. This paper describes the results of a series of combined static and random dynamic load tests simulating the expected ascent loads during the first flight. The tests were performed to ensure the integrity of the TPS remaining undensified in the wing and midfuselage region before the first flight. All specimens tested survived an equivalent of 72 ascent missions with residual strengths exceeding the original proof loads, indicating that the undensified tiles had sufficient strength to withstand ascent loads.

Introduction

THE Shuttle Orbiter is basically a conventional aluminum aircraft structure and as such must be insulated to prevent the skin temperature from exceeding 177°C (350°F) during reentry. The Thermal Protection System (TPS) used on the undersurface of the Orbiter consists of several thousand nearly square ceramic tiles with side dimensions on the order of 15.2 cm (6 in.) or less. The tiles are bonded to sections of low modulus felt material, which are in turn bonded to the skin of the Orbiter. The flexible felt material acts as a Strain Isolator Pad (SIP), permitting relative motion between the aluminum substructure and the tiles which reduces strains in the brittle tiles. To insure the integrity of the installed tile/SIP units, each is given a proof test consisting of a static load sufficient to produce a tensile stress equal to at least 125% of the expected maximum service stress in the tile and SIP. It is possible that the proof test itself could cause unacceptable damage to the TPS. To evaluate possible damage, acoustic emissions which occur during the test are monitored. The units which fail the proof test either by separating from the Orbiter or by exceeding a given level of acoustic emissions during the test are replaced with units strengthened in the tile in the region near the interface to the SIP.[1,2] The original TPS configuration exhibited a weakness in this region because of stress concentrations which occurred due to the discrete load transfer mechanism through the SIP.[3] The tile was strengthened at the interface by applying a ceramic liquid slurry to the tile bonding surface. The slurry fills the voids between fibers in the porous tile and on drying provides a densified region with sufficient strength to support the stress concentrations. Because of cost and schedule considerations, several thousand tiles which passed the proof test were not removed and remained undensified before the first flight.

The tiles experience a variety of loads during ascent. These include: main engine and solid rocket motor ignition overpressures during liftoff; substructure motions due to engine vibrations and aerodynamic loadings; direct acoustic pressure loads caused by boundary-layer noise; differential pressures due to shock passage, aerodynamic gradients and gust loads; and tile buffeting due to vortex shedding from connecting structure. Most of these loads are dynamic, rather than steady, raising the question of the low-cycle fatigue strength of the undensified TPS[4,5] when subjected to the random dynamic loading at stress levels equal to or below the maximum stress level established as acceptable by the static proof test. This paper describes the results of a series of base driven random dynamic load tests of TPS. The results were used to ensure the integrity of the undensified TPS prior to the first flight in the wing and midfuselage region shown in Fig. 1. The number of specimens and the load ranges investigated were limited, since the intent of the tests was not to provide an exhaustive dynamic response and fatigue study of the TPS, but rather to obtain an evaluation of the expected behavior of the TPS under dynamic loading during ascent to clear the tiles for the first flight of the Shuttle.

Test Specimens

The test specimen was designed to provide the desired loads, substructure deformations, and attachments needed for the various tests discussed in the next section. This section provides a detailed description of the TPS test fixture and the assembled specimen.

TPS Description

The TPS test specimen is composed of a ceramic tile with a needled (nonwoven) Nomex felt pad 0.41 cm (0.160 in.) thick-bonded to the uncoated face of the tile using a room temperature curing silicone rubber adhesive designated RTV-560. The tile is a aectangular parallelepiped, 15.2 cm^2 (6.0 $in.^2$) with a density of 144 kg/m^3 (9 lbm/ft^3), designated LI-900 Reuseable Surface Insulation (RSI). The RSI is composed of compacted silicon fibers bound together by colloidal silica fused at temperatures reaching 1320°C (2400°F). The tiles are

Presented as Paper 82-0790 at the AIAA/ASME/ASLE/AHS 23rd Structures, Structural Dynamics and Materials Conference, New Orleans, La., May 10-12, 1982; submitted July 26, 1982; revision received Oct. 12, 1983. This paper is declared a work of the U.S. Government and therefore is in the public domain.

*Aerospace Research Manager, Structures and Dynamics Division. Associate Fellow AIAA.

†Aerospace Engineer, Structures and Dynamics Division. Member AIAA.

‡Aerospace Engineer, Structures and Dynamics Division.

§Aerospace Engineer, Acoustics and Noise Reduction Division.

coated on five sides with reaction-cured glass consisting of silica, boron oxide, and silicon tetraboride. The coating is sprayed on the tile faces and glazed at 1090°C (2000°F). Tile mass is 128 g (0.28 lbm) for the wing region test tiles and 117 g (0.26 lbm) for the midfuselage region test tiles. Tile filler bars, composed of strips of coated Nomex felt slightly thicker than the SIP, are bonded to the structural surface of the Orbiter between tiles to prevent direct heat radiation or convection to the skin. These filler bars are included as a component of the test specimen and, as on the rest of the Orbiter, are bonded to the aluminum substrate only. A schematic of the test specimen indicating the relative location of each component is shown in Fig. 2.

Fixture Description

A detailed illustration of the test fixture is given in Fig. 3. The fixture consists of a 0.16-cm (0.063-in.) thick aluminum plate with a 25×25 cm (10×10 in.) planform riveted to five thick-walled aluminum tubes. The fixture was designed in such a way that after the tile/SIP unit is bonded to the plate, the plate can be deformed to a shape typical of the substructure deformations expected in the Orbiter skin in either the wing or midfuselage region of interest. Bolting the tubes to a rigid base plate with shims under alternate tubes causes the plate to deform to an approximate sine wave with the peak-to-peak wave amplitude given by the shim thickness. The half wavelength is governed by the 5.26 cm (2.07 in.) tube spacing.

Tile/Fixture Assembly

The fixture surfaces on which the specimens are bonded are first chemically etched, sprayed with a protective primer (Koropon), and vacuum baked to remove all volatiles. The tile and SIP are bonded to the test fixture with the tile diagonals parallel to the edge of the test fixture as shown in Fig. 3. The tile is located on the test fixture so that one corner of the SIP is over the centerline of one of the tubes. A circular aluminum 0.13-cm (0.05-in.) thick disk with a diameter of 10.2 cm (4.0 in.) is bonded to the top of the tile using epoxy adhesive to provide a load attachment point. The attachment point at the center of the disk is located 1.3 cm (0.5 in.) from the center of the tile measured along a tile diagonal perpendicular to the tube axes. Preliminary tests showed that a tension load in excess of 0.31 kN (70 lbf) could be applied to the top plate before the tile coating failed. A specimen in sequential stages of fabrication is shown in Fig. 4.

Test Procedure

A series of tests was performed on each specimen. To begin, the specimens were proof tested to determine their acceptability and to condition them so they had the same characteristics as the TPS just prior to first flight liftoff. Next, the specimens were subjected sequentially to two sets of combined static and random dynamic loads which are assumed to simulate conditions expected during ascent between the time transonic speeds are attained and occurrence of maximum dynamic pressures. At the conclusion of the dynamic tests, the tiles were reproofed to determine any change in SIP stiffness. Finally, the specimens were given a tensile test-to-failure to determine residual strength. The procedures followed for each type of test are described in this section.

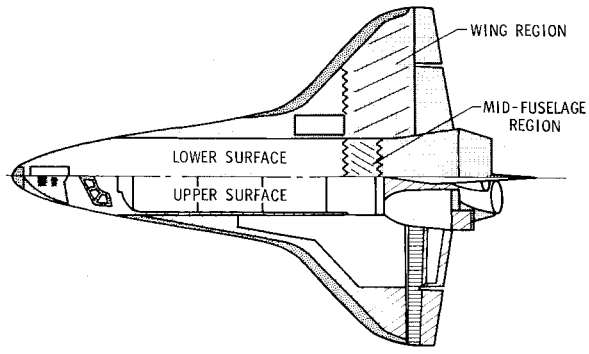

Fig. 1 Location on Orbiter of undensified tiles considered in test program.

Proof Test

A proof test was conducted on each specimen prior to its acceptance for structural testing in accordance with techniques approved for proof testing TPS on the Orbiter. The test involved applying uniform normal tension and compression loads to the TPS sufficient to impose an average stress on the SIP at least 25% greater than the static equivalent stress expected during ascent on the first flight for the TPS at locations of interest. Loads were applied to the face of the tile by a vacuum chuck attached to a pneumatic jack. The jack movement was controlled by an automatic pressure regulator system which imposed a preprogrammed load/time profile. A load cell measured the force applied to the tile. Acoustic emission transducers were located at the four corners of the tile. The acoustic emission test equipment was calibrated using a standard transducer with characteristics almost identical to the standard used during installation of tiles on the Orbiter. Acoustic emission data, loads, and displacements were recorded during the test.

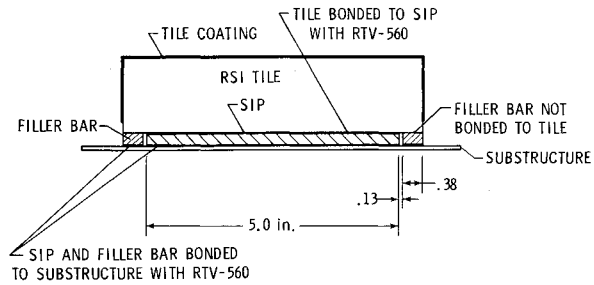

Fig. 2 Description of TPS. Dimensions are in in.

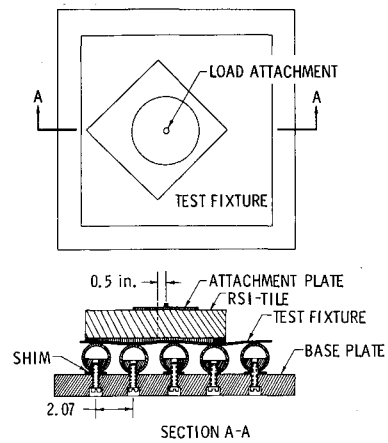

Fig. 3 Description of test fixture. Dimensions given in in.

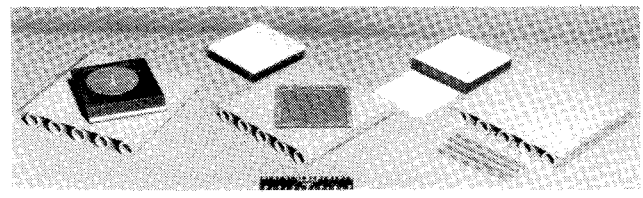

Fig. 4 Specimen in sequential stages of fabrication.

Specimens were accepted for testing if no separation between the tile and SIP occurred and the acoustic counts recorded during the tensile phase of the proof test did not exceed a specified value at each of several load levels. A typical 55 kPa (8 psi) proof test stress-displacement curve is shown in Fig. 5. The load/time profile included constant load applications during which the SIP exhibited a pronounced creep as evident in the figure. Following a successful proof test, the tile was wiped with alcohol to identify any cracks in the tile coating. Specimens failing the proof test were rejected or used for preliminary test runs. After the specimens had been subjected to the random dynamic loads discussed in the next section, they were each reproofed to determine their altered stress-displacement properties and to determine if they would still pass the proof test. The same proof procedure and acoustic counts criteria were used before and after the dynamic tests. Additional details are given in Ref. 6.

Random Dynamic Tests

The critical load conditions on the TPS during ascent occur between the time the Orbiter reaches transonic speeds (approximately 40 s after liftoff) and the time the Orbiter experiences maximum dynamic pressure (approximately 65 s after liftoff). During this critical time, the TPS in the wing and midfuselage region experiences substructure deformation, shock passage aerodynamic gradients which can cause a net tensile force and moment on the tile, and random acoustic loads transmitted to the tile from the Orbiter base structure. The experimental procedures used to apply approximations to these loads and the test instrumentation are described in this section.

Substrate Deformation

The base fixture is designed to give two different substructure deformation configurations, depending on which location of the Orbiter is being investigated. In the wing region, the area of interest is expected to have a half-wavelength substructure deflection of approximately 5.26 cm (2.07 in.), while in the midfuselage region the half-wavelength is expected to be approximately 10.5 cm (4.14 in.). These wavelength dimensions are dictated by local skin-stringer spacing of the Orbiter substructure. Although the stringer spacing is closer in regions of interest in the wing than in those of the midfuselage, the maximum amplitude expected in the wing region of 0.038 cm (0.015 in.) is greater than that in the midfuselage region of 0.02 cm (0.008 in.).

Random Load Spectra

The load spectrum during a given mission cycle is approximated using two base drive spectra in the normal direction. The two spectra are shown in Fig. 6 for both the wing and midfuselage regions. Procedures for developing the applied acceleration spectra of Fig. 6 are discussed in Ref. 7. Spectrum A contains the substructure dynamic response expected due to a combination of an aerodynamic gradient, which represents the condition when a shock is ahead (upstream) of the tile, plus a buffet load and has power levels such that the total G_{rms} is 27.0 for the wing region and 26.3 for the midfuselage region. Spectrum B contains the response expected due to a combination of a stationary shock on a tile plus a buffet load and has power levels such that the total G_{rms} is 21.4 for the wing region and 20.0 for the midfuselage region. The frequency ranges are constrained to 15 Hz by the displacement capability of the shaker table at the low end and are cut off on the high end at 1000 Hz because of power limitations; however, no significant system response is expected outside of this range. Previous sinusoidal dynamic tests performed on similar TPS[8,9] and analyses[10] indicated that the fundamental natural response frequencies of the tile/SIP units varied with displacement amplitude since SIP stiffness and damping responses are highly nonlinear. In the absence of static tension, the tile/SIP unit natural frequencies had an average of about 100 Hz. Thus, the power spectra used in these tests encompassed the expected resonant response frequencies of the specimens.

Static Loads and Moments

The total load level for a particular series of tests is controlled by the level of the static load component applied to the top of the tile at the attachment point. Two static load levels were applied during a mission cycle. The relationship between the applied static loads and the random dynamic power spectrum levels is given in Fig. 7. The maximum static load always occurs simultaneously with the application of the minimum power spectrum level for both the wing and midfuselage regions. A low-mass flexible cord is used to apply the static load component as shown in Fig. 8. The tension load applied to the flexible cord is time sequenced with the power spectrum levels. Since that attachment point lies off the tile center (Fig. 3), the load applies a moment as well as a tension load to the TPS. The combination of tension, moment, and substructure deformation causes the maximum static tensile stress to occur close to a corner of the SIP.

Mission Cycle Time

Maximum loading conditions during ascent were assumed to occur for 25 s, which encompasses the critical time duration. Each specimen was tested for ½ h, the approximate equivalent of 72 ascent missions. This test time was chosen to account for the uncertainties in load predictions, the variability of both material properties and fabrication, and installation techniques, and also was chosen since many tiles were scheduled to remain undensified for up to five flights.

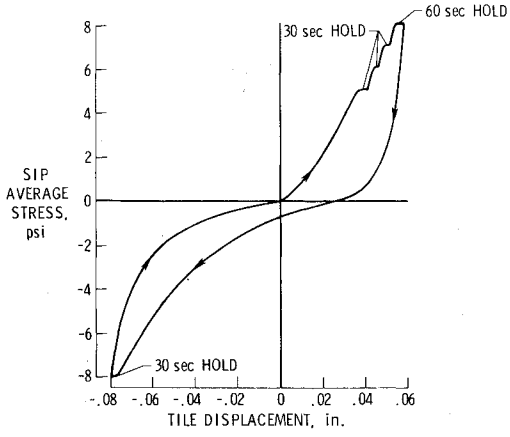

Fig. 5 Typical stress-displacement relationship for 55 kPa (8 psi) proof test of TPS specimen.

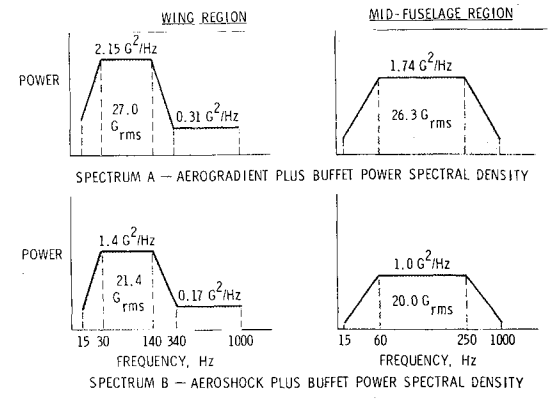

Fig. 6 Random vibration spectra for TPS specimens. Power increased or decreased at constant rate of +6 dB/oct.

Control System and Instrumentation

The schematic in Fig. 8 shows the apparatus used to control the combined loading in the tests. The prescribed broadband random acceleration of the tile base plate in the normal direction was provided by a 133 kN (30,000 lbf) electromagnetic shaker. An automatic drive control system with a random noise generator shaped the spectrum of the input signal to the shaker to get the desired spectrum measurement at the base plate of the system assembly. A dummy specimen was used to calibrate the input signal. The resultant drive signal was recorded with timed level changes on analog tape and used to drive every tile which required the spectrum. Thus, each specimen simulating a given location on the Shuttle was driven by the same random load spectra. The drive signal controlling the base acceleration was clipped to prevent accelerations greater than three times the driving G_{rms}. After the tiles were bonded to the fixture and the fixture bolted to the base plate using the appropriate shims to simulate the substructure deflection, the tiles were instrumented as shown in Fig. 9. Eight accelerometers attached to thin plastic load distribution pads were bonded to the tile at the locations shown. In addition, sections of 0.013 cm (0.005 in.) aluminum foil were bonded to the tile coating on the upper surface to act as targets for four proximity deflectometers. The combined mass of the instrumentation and top plate fixture was 28.6 g (0.063 lbm). The tile mass is 128 g (0.28 lbm) for the wing and 117 g (0.26 lbm) for the midfuselage. After instrumentation of the tiles, the base plate was bolted to the head of the shaker. To combine the steady-state tensile load with the dynamic loads discussed earlier, the flexible cord was attached to the metal plate bonded to the top of the tile. The tension load was controlled with a servo control system triggered by a signal from another channel of the drive tape so that the static tension level was varied simultaneously with input acceleration. During each test, all response signals were recorded on analog tape and displayed appropriately to monitor overall levels. Video recordings and high speed pictures were also taken at intervals during each test.

The major parameters and specimen dimensions for both the wing and midfuselage test program are given in Table 1.

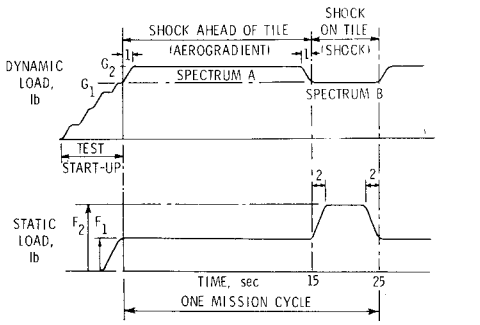

WING					MID-FUSELAGE				
σ_{MAX} kPa (psi)	F_1 N (lb)	F_2 N (lb)	G_1	G_2	σ_{MAX} kPa (psi)	F_1 N (lb)	F_2 N (lb)	G_1	G_2
44.1 (6.4)	22.2 (5)	71.2 (16)	21.4	27.0	33.1 (4.8)	22.2 (5)	151.2 (34)	20.0	26.3
50.3 (7.3)	26.7 (6)	97.9 (22)	21.4	27.0	37.9 (5.5)	22.2 (5)	182.4 (41)	20.0	26.3

Fig. 7 Static and dynamic load sequence per simulated mission for TPS specimens.

Ultimate Tension Tests

To determine the residual strength of the specimens after exposure to the mission fatigue tests and the second proof test, the tiles were subjected to a static tensile test-to-failure. The tests were conducted in a constant displacement rate test machine at 0.13 cm/min (0.05 in./min). The tile assembly was mounted on a base plate without shims and the plate clamped to the moveable crosshead of the test machine. An aluminum plate bonded to the top of the tile was attached to the stationary crosshead of the machine through a load cell and a spherical swivel. A 2.2 kN (500 lbf) tension load cell was used to measure the applied load. Specimen displacement was measured using four displacement gages located at the midsurface of each tile side. The displacement measurements

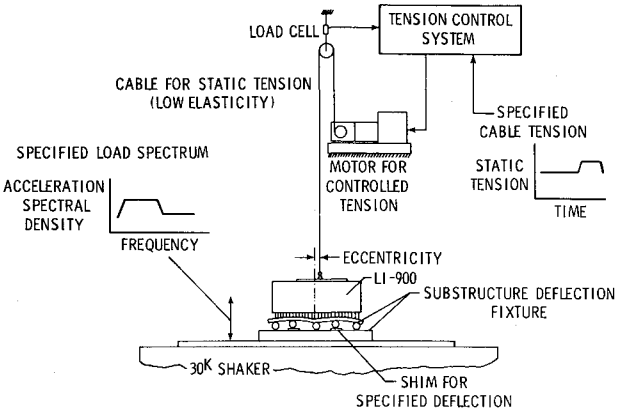

Fig. 8 Schematic of the random dynamic load test setup.

Table 1 Summary of test parameters

Parameter	Wing region	Midfuselage region
Tile thickness, cm (in.)	3.18 (1.25)	2.79 (1.10)
Tile mass, g (lbm)	128 (0.28)	117 (0.26)
Instrumentation and top plate mass, g (lbm)	28.6 (0.063)	28.6 (0.063)
Proof test level, kPa (psi)	55 (8)	41 (6)
Substructure deflection amplitude, cm (in.)	0.038 (0.015)	0.020 (0.008)
Substructure deflection half-wavelength, cm (in.)	5.26 (2.07)	10.52 (4.14)
Tension cord offset along diagonal, cm (in.)	1.3 (0.5)	1.3 (0.5)
Time/mission cycle, s	25	25
Total test time (72 ascent missions), h	½	½
Min/max load spectra, G rms	21.4/27.0	20.0/26.3
Maximum static load levels (nominal maximum stress), N (lbf)	71 (16)	151 (34)
	98 (22)	182 (41)

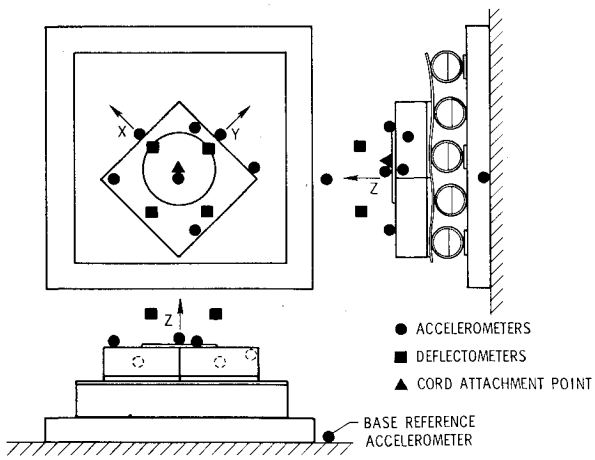

Fig. 9 Instrument sensor locations.

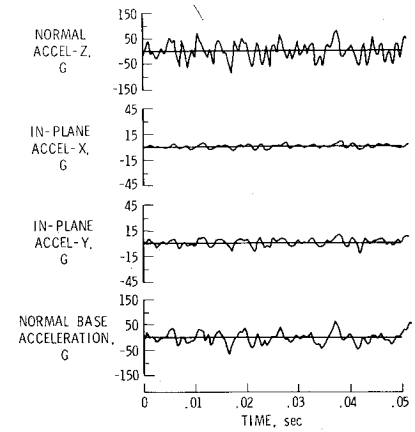

Fig. 10 Typical tile response histories under random base excitation with a static tension load applied.

were made between the top surface of the tile and the aluminum plate substructure. The specimens were tested to failure with a tensile load applied to the center of the tile. Load and displacement data were recorded using *x-y* recorders.

Data Analysis

The analog tile response data stored on magnetic tape was processed to produce digital tapes, each of which contained time and data channels. These digital tapes provided the source data for subsequent detailed analyses of the tile response characteristics. These analyses included: 1) computed summary statistics (maximum, minimum, mean, rms, standard deviation, skew) for each channel and provided time histories; 2) application of a time series analysis program to compute power spectral densities, cross-spectral densities, coherences, transfer functions, and cumulative distribution functions for specified data channels; 3) computation of the probability density and cumulative distribution function for the positive peaks (compression), negative peaks (tension), and total peaks associated with each data channel; and 4) derivation of tile center-of-gravity (c.g.) motions by applying the transformation equations relating c.g. motion to the actual measured accelerations at each accelerometer location.

The above analyses were performed for all of the tile acceleration measurements, the input normal base acceleration, and the derived (c.g.) accelerations. Transfer functions, cross-spectral densities, and coherences were computed between the following: the measured tile c.g. acceleration response and input acceleration; the derived c.g. acceleration response and input acceleration; and both measured and derived lateral tile acceleration responses relative to tile vertical acceleration response. These computations were performed for three mission cycles within each test and for both "high" and "low" static load conditions. The mission cycles selected for analyses were 2, 35, and 72 missions. Output of the analyses included both listings and plots of the desired tile response parameters.

Discussion of Results

Dynamic Response

The basic characteristics of tile response to random base excitation are illustrated by the response histories in Fig. 10. This figure shows the base excitation and the corresponding tile acceleration response in the normal and in-plane directions. The tile response is nonlinear and is characterized by relatively large negative acceleration peaks, which result in tension in the SIP. These peaks are significantly larger than the corresponding compression peaks. This type of response behavior is important in the consideration of the fatigue properties of the tile/SIP system.

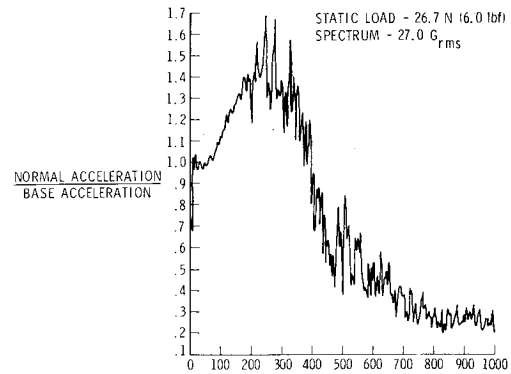

a) wing region.

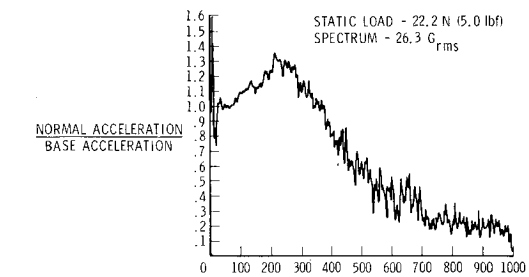

b) midfuselage region.

Fig. 11 Typical vertical response transfer function for low-tension condition.

Figure 10 also indicates that an acceleration response occurs along the two in-plane axes, each having a much lower amplitude response than the response in the normal direction. The difference in in-plane response is probably due to the non-homogeneous properties of the SIP material.[11] The derived c.g. accelerations of the tile, which are not shown, were found to be virtually identical to the measured accelerations. Typical overall normal response characteristics of the tiles in the wing and midfuselage regions are given by the transfer functions of Figs. 11 and 12, respectively. These functions were obtained from analyses of 10-12 s of tile response. They represent the ratio of tile c.g. normal response to base excitation as a function of frequency. Figures 11a and 12a are the transfer functions for the wing region obtained for tension loads of 26.7 N (6.0 lbf) and 97.9 N (22.0 lbf) and base drive spectrum acceleration levels of 27.0 and 21.4 G_{rms}, respectively. Figures 11b and 12b are the transfer functions for the midfuselage region and correspond to tension loads of

22.2 N (5 lbf) and 182 N (41 lbf) and spectrum acceleration levels of 26.3 and 20.0 G_{rms}. Both sets of transfer functions show that for the low tension loads (Fig. 11), the resonant response occurs in the 360-500-Hz range for the wing region (Fig. 12a) and the 520-680-Hz range for the midfuselage region (Fig. 12b). Thus, the tension loads tend to increase the tile response frequencies by an amount dependent upon tension load, spectrum level, and tile mass. It also acts to increase the value of the transfer function at tile resonance. From the data shown in Figs. 11 and 12, and additional data obtained during the tests, an increase in the static tension loads and spectrum levels increases the transfer function by as much as a factor of two. Thus, the presence of tension loads significantly alters dynamic response characteristics of the tile/SIP system. Coherence analyses between the normal acceleration response and base drive input acceleration indicated that tile responses were fully coherent over the frequency range investigated.

For a fatigue analysis, the direction of peak acceleration occurrences is very significant. A typical probability distribution of peak normal acceleration response levels is given in Fig. 13. The zero value in the distribution at zero acceleration is due to the peak counting procedure which ignores peaks below 1% of maximum. This was a result of the practical limitations inherent in defining low-level peaks which are often masked by signal noise. The distribution displays a double peak appearance indicative of a narrow-band response. Relatively high negative acceleration peaks (tension peaks) do occur infrequently; however, they must be considered in the assessment of the fatigue life.

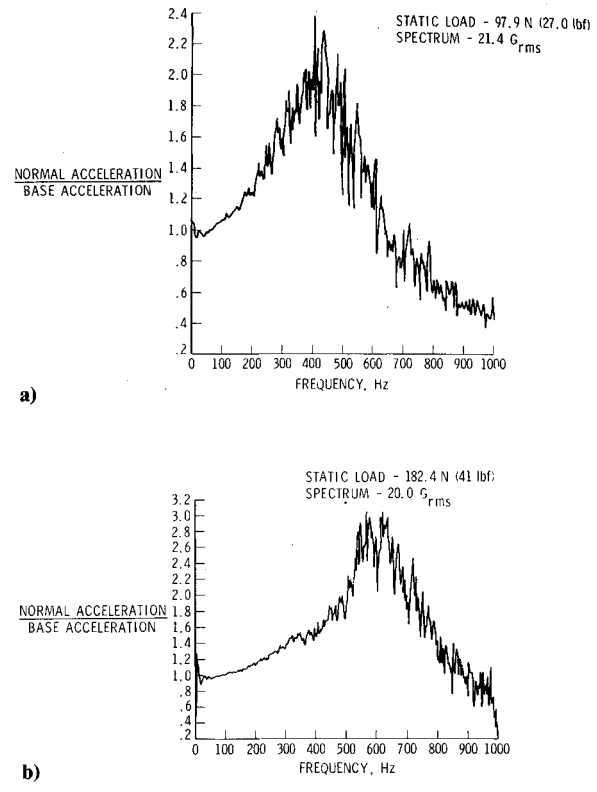

Fig. 12 Typical vertical response transfer function for high tension condition: a) wing region; b) midfuselage region.

Specimen Residual Properties

Reproof Tests

On reproof, all specimens successfully supported the original proof test load and only two wing region specimens failed the acoustic emission criteria. The excess noise detected on these two specimens was thought to be due to surface cracks in the tile coating caused by removing the instrumentation and flexible cord attachment plate. Thus, the failure of the two specimens to pass the acoustic emission criteria during the reproof was not considered to have any significance to the tiles on the Orbiter.

Stress-Displacement Properties

The effect of the dynamic fatigue tests on the stress-displacement properties of the specimen can be seen in Fig. 14, where typical proof stress-displacement curves obtained before and after the dynamic tests are shown. The initial proof test curves (shown by the solid lines) indicate that a relatively uniform extension or contraction of the SIP occurs during the proof test. After the dynamic tests, the reproof test curves (shown by the dashed lines) indicate that the SIP near the side of the tile nearest the flexible cord attachment extends or contracts considerably more for a given stress level than does the SIP near the other side of the tile. This indicates that the eccentric loading of the specimen during the dynamic tests has a permanent effect on the SIP properties. The dynamic tests also result in the specimen having a more extensive low-modulus region for low stress levels and thus a larger displacement for a given stress level. The growth of the low-modulus region of the SIP which occurs with repeated dynamic loading could cause excessive tile looseness and should be considered in evaluating the useful lifetime of the

Table 2 Specimen residual strength after random dynamic load test

Proof levels	Nominal maximum dynamic stress test level, kPa (psi)		Static ultimate strength after dynamic tests, kkPa (psi)	
Wing region	44	(6.4)	93.8	(13.6)
55 kPa (8 psi)	44	(6.4)	86.9	(12.6)
	44	(6.4)	80.7	(11.7)
	44	(6.4)	75.8	(11.0)
	50	(7.3)	98.6	(14.3)
	50	(7.3)	84.1	(12.0)
	50	(7.3)	80.7[a]	(11.7)
	50	(7.3)	62.0[a]	)9.0)
Midfuselage region	33	(4.8)	106.2	(15.4)
41 kPa (6 psi)	33	(4.8)	96.5	(14.0)
	33	(4.8)	91.7	(13.3)
	33	(4.8)	83.4	(12.1)
	38	(5.5)	106.2	(15.4)
	38	(5.5)	103.4	(15.0)
	38	(5.5)	93.8	(13.6)
	38	(5.5)	81.3	(11.8)

[a] Failed acoustic admission after dynamic load test.

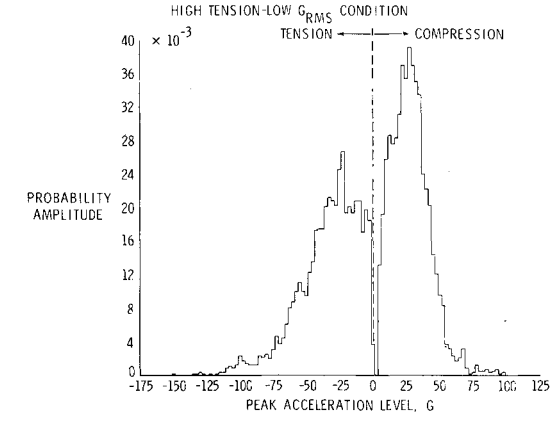

Fig. 13 Typical probability distribution of tile acceleration peaks for high tension condition in the midfuselage region.

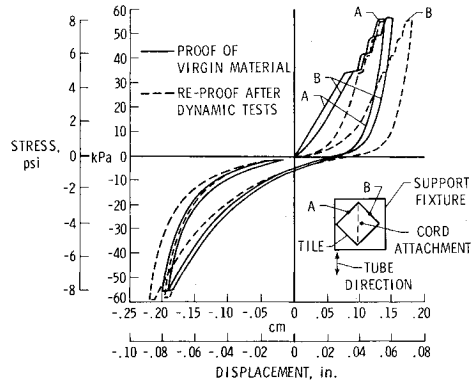

Fig. 14 Stress-displacement curves for typical TPS wing specimen before and after dynamic tests.

TPS. This result is a consequence of the character of the SIP material and thus can be expected to also occur for densified tiles.

Residual Tensile Strength

Residual tensile strength of the specimens after the dynamic fatigue tests and the reproof test are tabulated in Table 2. All the specimens exhibited residual static tensile strengths greater than their original proof loads. The specimens for the wing and midfuselage regions had an average residual strength of 83 kPa (12.0 psi) and 95 kPa (13.8 psi), respectively. These residual strengths are as high or higher than average static tensile strength values obtained on large numbers of virgin tiles. Thus, the 72-mission cycle dynamic fatigue tests did not have any appreciable effect on the static ultimate tensile strength of the undensified TPS tile system.

Concluding Remarks

This paper describes the results of a series of combined static and random dynamic load tests simulating the expected ascent loads during the Shuttle Orbiter first flight. The tests were conducted on Thermal Protection System laboratory specimens which passed the proof test and thus would have remained undensified on the vehicle. The tests were performed to ensure the integrity of undensified TPS remaining in the wing and midfuselage region prior to the first flight. All specimens for both the wing and midfuselage regions survived an equivalent of 72 ascent missions and exhibited residual static strength greater than their original proof loads. These results indicate that the undensified tiles had sufficient strength to withstand ascent loads during the first flight.

Dynamic response data indicated that tile normal response is nonlinear and is characterized by relatively high tension peaks in the SIP, which are generally significantly larger than the compression peaks. This fact should be accounted for in estimations of fatigue life. The amplitude response characteristics of the tiles were found to be dependent upon tension load, spectrum level, and added tile mass. The data indicated that in the frequency range of tile resonance, response accelerations can exceed by a factor of three the base drive acceleration levels. In-plane responses, although present, were of much lower amplitude than the corresponding normal response levels. The data further indicated that application of tension loads to the tiles produced substantial changes in tile response behavior, namely an increase in tile resonant frequency and amplitude response levels.

Some degradation of the SIP stiffness was evident after the 72 simulated ascent missions. Repeated dynamic loading could cause excessive tile looseness and should be considered in evaluating the useful lifetime of the TPS. This behavior is caused by the character of the SIP material and thus can be expected to occur for densified TPS as well.

References

[1] Cooper, P. A. and Holloway, P. F., "The Shuttle Tile Story," *Astronautics & Aeronautics*, Vol. 19, pp. 24-36. Jan. 1981.

[2] Korb, L. J., and Clancy, H. M., "Shuttle Orbiter Thermal Protection System—A Material and Structural Overview," *Material and Process Applications—Land, Sea, Air, Space; Proceedings of the 26th National Symposium and Exhibition,* Society for the Advancement of Material and Process Engineering, 1981, pp. 232-249.

[3] Prabhakaran, R. and Cooper, P. A., "Photoelastic Tests on Models of Thermal Protection System for Space Shuttle Orbiter," NASA TM 81866, Aug. 1980.

[4] Sawyer, J. W. and Cooper, P. A., "Fatigue Properties of Shuttle Thermal Protection System," NASA TM 81899, Nov. 1980.

[5] Phillips, E. P., "Tension-Tension Fatigue Behavior of the Space Shuttle Strain-Isolation-Pad Material," NASA TM 83183, Aug. 1981.

[6] Sawyer, J. W., "Effect of Load Eccentricity and Substructure Deformations on Ultimate Strength of Shuttle Orbiter Thermal Protection System," NASA TM 83182, Sept. 1981.

[7] Muraca, R. J., Coe, C. F., and Tulinius, J. R., "Shuttle Tile Environment and Loads," AIAA Paper 82-0631, May 1982.

[8] Leatherwood, J. D., and Gowdey, J. C., "Mission Load Dynamic Tests of Two Undensified Space Shuttle Thermal Protection System Tiles," NASA TM 83148, June 1981.

[9] Miserentino, R., Pinson, L. D., and Leadbetter, S. A., "Some Space Shuttle Tile/Strain-Isolator-Pad Sinusoidal Vibration Tests," NASA TM 81853, July 1980.

[10] Housner, J. M., Edighoffer, H. H., and Park, K. C., "Nonlinear Dynamic Response of a Unidirectional Model for the Tile/Pad Shuttle Thermal Protection System," NASA TM 81901, Nov. 1980.

[11] Sawyer, J. W., "Mechanical Properties of the Shuttle Orbiter Thermal Protection System Strain Isolator Pad," AIAA Paper 82-0789, May 1982.